phosphate phosphatase also purified from baker's yeast by Millay and Houston (1973) exactly corresponds in molecular weight, 38,000, to the molecular weight of the phosphatase from the UGA nonsense mutant which defines the region comprising the "phosphatase globule" of the bifunctional *hisB* enzyme described by Houston (1973b).

References

Ahmed, A., Case, M. E., and Giles, N. H. (1964), *Brookhaven Symp. Biol. 17,* 53–63.

Ames, B. N. (1957), *J. Biol. Chem. 228,* 131.

Ames, B. N., and Hartman, P. E. (1962), *in* The Molecular Basis of Neoplasia, Austin, Tex., University of Texas Press, p 322.

Ames, B. N., and Martin, R. G. (1964), *Annu. Rev. Biochem. 33,* 235–258.

Bernardi, G. (1971), *Methods Enzymol. 22,* 325.

Brady, D. R., and Houston, L. L. (1973), *J. Biol. Chem. 248,* 2588–2592.

Cleland, W. W. (1970), *Enzymes, 3rd Ed. 2,* 1–65.

Davis, B. J. (1964), *Ann. N. Y. Acad. Sci. 121,* 404.

Fink, G. R. (1964), *Science 146,* 525–527.

Hartman, P. E., Hartman, Z., Stahl, R. C., and Ames, B. N. (1971), *Advan. Genet. 16,* 1–34.

Hedrick, J. L., and Smith, A. J. (1968), *Arch. Biochem. Biophys. 126,* 155–164.

Houston, L. L. (1973a), *J. Bacteriol. 113,* 82–87.

Houston, L. L. (1973b), *J. Biol. Chem. 248,* 4144–4149.

Houston, L. L. (1973c), *J. Bacteriol. 116,* 88–97.

Houston, L. L., and Graham, M. E. (1974), *Arch. Biochem. Biophys. 162,* 513–522.

Hjerten, S. (1962), *Arch. Biochem. Biophys. Suppl. 1,* 147–151.

Klopotowski, T., and Wiater, A. (1965), *Arch. Biochem. Biophys. 112,* 562–566.

Layne, E. (1957), *Methods Enzymol. 3,* 447–454.

Loper, J. C. (1961), *Proc. Nat. Acad. Sci. U. S. 47,* 1440–1450.

Loper, J. C., Grabnar, M., Stahl, R. C., Hartman, Z., and Hartman, P. E. (1964), *Brookhaven Symp. Biol. 17,* 15–52.

Lowry, O. H., Rosebrough, N. J., Farr, A. L., and Randall, R. J. (1951), *J. Biol. Chem. 228,* 265–275.

Martinez-Carrion, M., Turano, C., Riva, F., and Fascella, P. (1967), *J. Biol. Chem. 242,* 1426–1430.

Millay, R. H., and Houston, L. L. (1973), *Biochemistry 12,* 2591–2596.

Peterson, A., and Sober, H. A. (1962), *Methods Enzymol. 5,* 1.

Ray, W. J. (1967), *Methods Enzymol. 11,* 490.

Ray, W. J., and Koshland, D. E. (1962), *J. Biol. Chem. 237,* 2493–2505.

Shaffer, B., Edelstein, S., and Fink, G. R. (1972), *Brookhaven. Symp. Biol. 23,* 250–270.

Shaffer, B., and Fink, G. R. (1969), *Genetics 61,* 54.

Vasington, F. W., and LeBeau, P. (1967), *Biochem. Biophys. Res. Commun. 26,* 153–160.

Weber, K., and Osborn, M. J. (1969), *J. Biol. Chem. 244,* 4406–4412.

Weil, L. (1965), *Arch. Biochem. Biophys. 110,* 57–68.

Westhead, E. W. (1965), *Biochemistry 4,* 2139.

Whitaker, J. R. (1963), *Anal. Chem. 35,* 1950.

Whitfield, H. J., Smith, D. W. E., and Martin, R. G. (1964), *J. Biol. Chem. 239,* 3288–3291.

Wiater, A., Hulanicka, D., and Klopotowski, T. (1971a), *Acta Biochim. Polon. 18,* 289–297.

Wiater, A., Klopotowski, T., and Bagdasarian, G. (1971b), *Acta Biochim. Polon. 18,* 309–314.

Wiater, A., Krajewska-Grynkiewicz, K., and Klopotowski, T. (1971c), *Acta Biochim. Polon. 18,* 299–307.

Molecular Kinetics of Beef Heart Lactate Dehydrogenase†

Uwe Borgmann, Thomas W. Moon, and Keith J. Laidler*

ABSTRACT: The dehydrogenation of lactate to pyruvate, catalyzed by beef heart lactate dehydrogenase, proceeds by an ordered ternary complex mechanism. A study has been made of the steady-state and pre-steady-state kinetics of the reaction in both directions, at various substrate and coenzyme concentrations, and over a range of temperatures (5–50°). Analysis of the results allowed eight rate constants to be determined, together with their enthalpies and entropies of activation. The concentration of active enzyme was also calculated from the kinetic results, and is consistent with the value obtained from the protein concentration and the molecular weight. The entropy changes during the course of the individual reactions suggest that the enzyme is most folded in the ternary complex. Biological implications of the results are considered, and it is noted that beef heart lactate dehydrogenase is particularly well suited for interconverting pyruvate and lactate at normal body temperature and at substrate concentrations commonly found in living systems.

Reactions catalyzed by lactate dehydrogenase and alcohol dehydrogenase have been studied extensively in the steady-state and the pre-steady-state (Holbrook and Gutfreund, 1973; for a review see Laidler and Bunting, 1973). The reactions are found to occur largely by an ordered ternary complex mechanism. The present paper describes an investigation of the pre-steady-state and steady-state kinetics of the beef heart lactate dehydrogenase system, over a range of temperature, and has allowed kinetic parameters to be obtained for eight elementary reactions.

By lowering the temperature to 15° and below, it is possi-

† From the Departments of Biology and Chemistry, University of Ottawa, Ottawa K1N 6N5, Canada. *Received May 22, 1974.* This work was supported by grants from the National Research Council of Canada.

ble to slow down the pre-steady-state processes to the point where an accurate study can be made in a stopped-flow apparatus. In contrast to adding inhibitors, this method of slowing down the reaction does not complicate the normal enzyme mechanism and can be used to extrapolate to higher temperatures on the basis of the Arrhenius law. Furthermore, by varying the temperature, it is possible to separate rate constants which are summed and are not multiplied by substrate concentrations. This technique has been used in the present work to calculate eight of the rate constants involved in the beef heart lactate dehydrogenase mechanism. In addition, the free energies, enthalpies, and entropies of activation have been obtained for eight reactions, and lead to interesting conclusions about conformational changes in the various elementary processes.

Theoretical

The reaction mechanism for lactate dehydrogenase can be represented as

$$E + A \underset{k_{-1}}{\overset{k_1[A]}{\rightleftharpoons}} EA \underset{k_{-2}}{\overset{k_2[B]}{\rightleftharpoons}} EAB \underset{k_{-3}[X]}{\overset{k_3}{\rightleftharpoons}}$$

$$EY \underset{k_{-4}[Y]}{\overset{k_4}{\rightleftharpoons}} E + Y$$

where A and B are NAD^+ and lactate, or their concentrations, and X and Y are pyruvate and NADH, or their concentrations. We are assuming that EAB and EXY are rapidly interconverted and, for simplicity, write EAB for EAB-EXY.

It is recognized that the above mechanism represents an oversimplification. Additional steps could have been included, for example, EAB $\rightleftharpoons$ EXY and conformational isomerizations of the type EA $\rightleftharpoons$ EA*. However, the present experimental data are found to be interpretable in terms of the above scheme. Inclusion of additional steps would have made interpretation of the results very cumbersome, since many different possibilities would have to be taken into account. These limitations should be borne in mind in considering the significance of the conclusions at which we arrive.

Pre-Steady-State Kinetics

The pre-steady state was followed in the direction lactate $\rightarrow$ pyruvate, and the discussion that follows relates to reaction in this direction. The pre-steady-state equations for an ordered ternary complex mechanism such as this have been worked out by Hijazi and Laidler (1973b). There are three kinetic intermediates, and according to a theorem due to Maguire *et al.* (1974) a triphasic exponential rise to the steady state is to be expected. In the present work only a single exponential was observed; this indicates that two of the steps in the above mechanism are too fast to be detected in the stopped-flow apparatus. As will be shown, k_3 must correspond to the slowest step in the pre-steady state ($k_3 \ll k_2[B]$) and is the only step observed. An equilibrium can thus be assumed between E, EA, and EAB

$$[EAB] = \frac{k_2[B][EA]}{k_{-2}} \quad (1)$$

and

$$[EA] = \frac{k_1[A][E]}{k_{-1}} \quad (2)$$

The total enzyme concentration $[E_0]$ is thus

$$[E_0] = [E] + [EA] + [EAB] + [EY] = [E](a) + [EY] \quad (3)$$

where

$$a = 1 + \frac{k_1[A]}{k_{-1}} + \frac{k_1k_2[A][B]}{k_{-1}k_{-2}} \quad (4)$$

The rate of change of [EY] with time is

$$d[EY]/dt = k_3[EAB] - k_4[EY] \quad (5)$$

whence

$$\frac{d[EY]}{dt} = \frac{k_1k_2k_3[E_0][A][B]}{k_{-1}k_{-2}(a)} - \left[\frac{k_1k_2k_3[A][B]}{k_{-1}k_{-2}(a)} + k_4\right][EY] \quad (6)$$

Integration and substitution for (a) leads to

$$[EY] = \text{const.}\,(1 - e^{-\lambda t}) \quad (7)$$

where

$$\lambda = \frac{k_1k_2k_3[A][B]}{k_{-1}k_{-2} + k_1k_{-2}[A] + k_1k_2[A][B]} + k_4 \quad (8)$$

Since $d[Y]/dt = k_4[EY]$, substitution and integration leads to

$$[Y] = \nu_{ss}t + Ce^{-\lambda t} + C' \quad (9)$$

where ν_{ss} is the steady-state velocity and C and C' are constants. With saturating concentrations of A, λ simplifies to

$$\lambda = \frac{k_3[B]}{(k_{-2}/k_2) + [B]} + k_4 \quad (10)$$

A plot of [Y] against time yields $\nu_{ss} + C'$, and λ can then be obtained by plotting log ($[Y] - C' - \nu_{ss}$) against time (Hijazi and Laidler, 1973a).

The concentration of X as a function of time is expressed in a similar manner as for Y; the value of λ is the same, but the values of the two constants are in general different. The formation of Y must show an initial lag, which is caused by the time required for the concentrations of the intermediates to reach steady-state levels. However, if (and only if) k_4 is rate limiting in the steady state the concentration of X might show an initially high rate of production ("initial burst").

In our experiments the reaction was monitored by observing the absorption at 340 nm; NADH absorbs at this wavelength whether or not it is bound to the enzyme. With no NADH or pyruvate present at the beginning of the measurements, the sum of the concentrations of NADH and E: NADH is thus equal to the concentration of pyruvate formed. The technique thus follows the production of the first product X.

In the experiments to be described, an initial burst was observed in the production of X, and this indicates that reaction 4 is rate limiting in the steady state. The constant λ is thus approximately

$$\lambda = \frac{k_3[B]}{(k_{-2}/k_2) + [B]} \quad (11)$$

Variation of [B] thus gives the constants k_3 and k_{-2}/k_2. The latter ratio is the concentration of B at half-maximal pre-steady-state velocities, and is analogous to the Michaelis constant in steady-state studies.

The observed hyperbolic relationship between λ and [B] proves that equilibrium is rapidly established as far as EAB;

if the slow step were reaction 2, λ would vary linearly with [B].

To summarize, the pre-steady-state studies prove that reaction 4 is the slow step in the steady state, and reaction 3 in the pre-steady state. The measurements also allow values of k_3 and k_{-2}/k_2 to be determined. The remaining kinetic constants are obtained from steady-state studies, in conjunction with the stopped-flow measurements.

Steady-State Kinetics

Steady-state rates were measured for the reaction occurring in both directions. The steady-state equations for the ordered ternary complex mechanism (Laidler and Bunting, 1973) lead to the following relationships for saturating coenzyme conditions. For the reaction lactate → pyruvate

$$\bar{V}_{max} = k_3k_4[E_0]/(k_3 + k_4) \quad (12)$$

$$K_{mB} = k_4(k_{-2} + k_3)/k_2(k_3 + k_4) \quad (13)$$

where K_{mB} is the Michaelis constant with respect to [B] (lactate). For the reverse direction pyruvate → lactate

$$\bar{V}_{-max} = k_{-1}k_{-2}[E_0]/(k_{-1} + k_{-2}) \quad (14)$$

$$K_{mX} = k_{-1}(k_{-2} + k_3)/k_{-3}(k_{-1} + k_{-2}) \quad (15)$$

Simplification is obtained by dividing each K_m by the corresponding V_{max}

$$K_{mB}/\bar{V}_{max} = (k_{-2} + k_3)/k_2k_3[E_0] \quad (16)$$

$$\frac{K_{mX}}{\bar{V}_{max}} = \frac{k_{-2} + k_3}{k_{-2}k_{-3}[E_0]} = \frac{1}{k_{-3}[E_0]} + \frac{k_3}{k_{-2}k_{-3}[E_0]} = C + D \quad (17)$$

The symbol C will be used to represent either $1/k_{-3}[E_0]$ or $k_3/k_{-2}k_{-3}[E_0]$, and D to represent the remaining term. The terms to which C and D actually relate are deduced on the basis of experiment, as discussed later. The ratio of eq 17 and 16 gives

$$(K_{mX}/V_{max})/(K_{mB}/V_{max}) = k_2k_3/k_{-2}k_{-3} \quad (18)$$

This ratio can be obtained from experiment, and the value of $C + D$ can be obtained either from $K_{mX}/\bar{V}_{max}$ or $K_{mB}/\bar{V}_{max}$, multiplied by $k_2k_3/k_{-2}k_{-3}$.

The experimental values of $C + D$ can then be plotted as an Arrhenius plot. Both C and D should be linear on such a plot, and a curve equal to the summation of two lines on the Arrhenius plot can be fitted to the data. These two lines can be labeled C and D, but it is not known which is which. The ratio C/D is equal to

$$\frac{C}{D} = \frac{k_{-2}}{k_3} \text{ or } \frac{k_3}{k_{-2}} \quad (19)$$

From steady-state data alone it is not possible to decide between the two possibilities; a procedure for deciding is considered later.

The value of k_1 can be obtained from steady-state measurements at saturating B and low A concentrations, as follows. With saturation by B, $\bar{V}_{max}$ is still given by (12) and K_{mA} is

$$K_{mA} = k_3k_4/k_1(k_3 + k_4) \quad (20)$$

The rate at low [A] is thus

$$v = V_{max}[A]/K_{mA} = k_1[E_0][A] \quad (21)$$

If the enzyme concentration is known k_1 can thus be determined. A similar procedure can be used to obtain k_{-4} from studies of the reverse reaction.

To summarize, the steady-state measurements alone allow one to determine the following. (1) $1/k_{-3}[E_0]$ and $k_3/k_{-2}k_{-3}[E_0]$, but one cannot determine which is which. When this is done (see later), $k_{-3}[E_0]$ and k_3/k_{-2} are known. (2) Measurements at low [A] and saturation with B lead to k_1. (3) Measurements at low [Y] and saturation with X lead to k_{-4} (in fact, as explained later, an alternative procedure was more satisfactory).

Combined Pre-Steady-State and Steady-State Data

The pre-steady-state data give k_3. Multiplication of k_3 by C/D and by D/C gives two values, one of which is equal to k_{-2}. Substitution back into the original equations for k_m/V_{max} [eq 16 and 17] for both of the possibilities gives two alternative estimates for $k_{-3}[E_0]$, $k_3/k_{-2}k_{-3}[E_0]$, and $k_2[E_0]$. Division of k_{-2} by $k_2[E_0]$ then gives two estimates for $k_{-2}/k_2[E_0]$. However, k_{-2}/k_2 was determined from the pre-steady-state data, and one can compare its temperature dependence with the two estimates for $k_{-2}/k_2[E_0]$. In this way, it is possible to determine which estimate of k_{-2}/k_2 is correct, *i.e.*, which terms C and D are equal to.

Further substitution then gives all the constants k_2, k_{-2}, k_3, and k_{-3}, and gives the value of $[E_0]$. Substitution of $[E_0]$ into the two V_{max} expressions (eq 12 and 14) then gives k_4 and k_{-1}.

Since k_1 and k_{-4} were determined independently (see above), all eight rate constants have been determined. From their temperature dependence the enthalpies and entropies of activation can be calculated, use being made of the relationships (Glasstone *et al.*, 1941; Laidler, 1965, 1969)

$$k = \frac{\mathbf{k}T}{h}e^{-\Delta G^{\ddagger}/RT} \quad (22)$$

$$= \frac{\mathbf{k}T}{h}e^{\Delta S^{\ddagger}/R}e^{-\Delta H^{\ddagger}/RT} \quad (23)$$

where $\Delta H^{\ddagger}$ is related to the experimental activation energy E_{act} by

$$\Delta H^{\ddagger} = E_{act} + RT, \quad (24)$$

k is the Boltzmann constant and h, Planck's constant.

Experimental Section

Materials. Beef heart lactate dehydrogenase (lot 63C-9540), lactate, pyruvate, NAD^+, and NADH were obtained from the Sigma Chemical Company. The lactate dehydrogenase was a crystalline suspension in ammonium sulfate; the ammonium sulfate was not dialyzed out since addition of this salt, to several times greater than the original concentration, was found to have no effect on the kinetics.

Kinetic Procedure. A Unicam SP-1800 spectrophotometer was used for the steady-state work, and the pre-steady state was followed using a Durrum-Gibson stopped-flow apparatus. Absorption was measured at 340 nm; as previously noted, this measures the pyruvate concentration. Most of the steady-state measurements were made over the temperature range from 5 to 50°; a Lauda Model-NB-D constant temperature bath was used, the temperature being checked with a Yellow Springs Model-43 telethermometer. Stopped-flow measurements were made from 0 to 15°, the pre-steady-state being too fast to follow at higher temperatures; the temperature was controlled by means of a Haake Model-KT-33 low-temperature circulator.

For the steady-state work the enzyme concentration was 0.25 mg/l.; for the stopped-flow measurements, the concen-

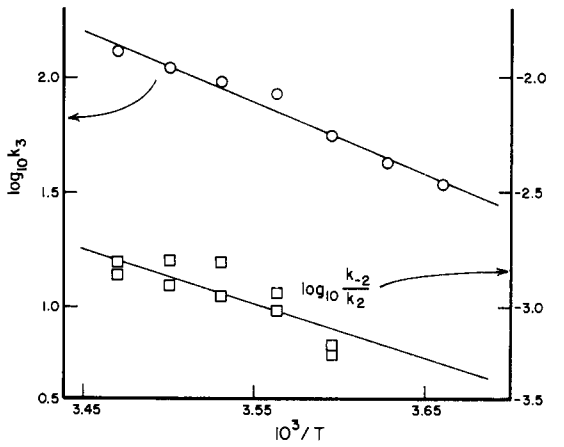

FIGURE 1: Arrhenius plots of k_3 (sec^{-1}) and k_{-2}/k_2 (M), obtained from the pre-steady-state measurements.

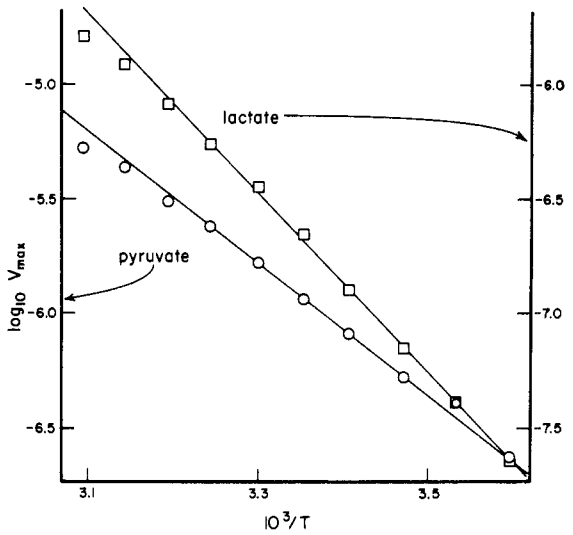

FIGURE 2: Arrhenius plots of the V_{max} values for the reactions in forward (lactate → pyruvate) and reverse directions; units of V_{max} are M sec^{-1}.

tration was 200 mg/l. The saturating concentrations of NAD^+ and NADH were determined to be 2 and 0.1 mM, respectively. All reactions were carried out at pH 7.4 in 0.05 M phosphate buffer.

The results were analyzed by means of Wilkinson plots of [substrate]/v against [substrate]. There is some substrate inhibition; only lower substrate concentrations were used in the calculations.

For the determination of k_1, the stopped-flow apparatus was used to measure the steady-state rates at high lactate (5 mM) and low NAD^+ (0.02 mM) concentrations at temperatures above 15°. Below 15° the K_m for NAD^+ is below 0.02 mM and lower concentrations of NAD^+ must be made.

Results

Stopped-Flow Measurements. The values of k_3 and k_{-2}/k_2, obtained in the stopped-flow studies as explained in the Theoretical section, are plotted logarithmically against $1/T$ in Figure 1. The values of k_{-2}/k_2 are more difficult to obtain accurately than values of k_3, and are more reliably obtained from the steady state; further calculations are made using values so obtained.

Steady-State Measurements. The maximum steady-state velocities in the two directions, $\vec{V}_{max}$ and $\overleftarrow{V}_{max}$, are

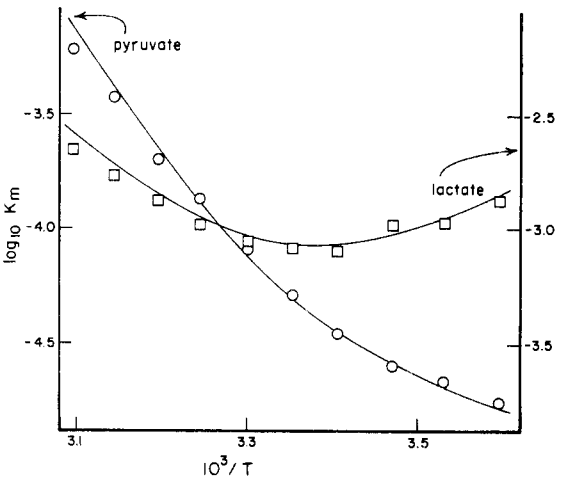

FIGURE 3: Logarithmic plots of K_m (M) against $1/T$ for the reactions in forward and reverse directions.

shown plotted logarithmically against $1/T$ in Figure 2. In both cases, straight lines are obtained, which suggests that each velocity is controlled primarily by one rate constant over the temperature range employed. As seen above, $\vec{V}_{max}$ is equal to $k_4[E_0]$, and we tentatively assume that $\overleftarrow{V}_{max}$ is equal to $k_{-1}[E_0]$; at present, we have no evidence for this.

The K_m values for lactate and pyruvate are plotted logarithmically against $1/T$ in Figure 3. The curves fitted to the data were calculated using expressions 13 and 15, the values for the individual rate constants being given in Table I. Plots of log $(k_2k_3/k_{-2}k_{-3})$ against $1/T$ gave a good straight line.

The values of log $(C + D)$ are plotted against $1/T$ in Figure 4. Values calculated both from $K_{mX}/\vec{V}_{max}$ and from $K_{mB}/\vec{V}_{max}$, multiplied by the values of $k_2k_3/k_{-2}k_{-3}$ obtained from the straight line in Figure 4, are shown. The diagram also shows two straight lines, one equal to C and the other to D, and their sum is represented by the curve in the diagram. The theoretical expressions for K_{mB} and K_{mX} (eq 13 and 15) suggest that the curvatures in these plots result from the summations of the same rate constants; the curvatures for the two sets of points in Figure 4 should therefore be the same. The consistency between the two sets of points, and their fit to the calculated curve, supports this interpretation.

If $C = 1/k_{-3}[E_0]$ and $D = k_3/k_{-2}k_{-3}[E_0]$ the value of C/D is equal to k_{-2}/k_3 (*cf.* eq 19). Multiplication by

TABLE I: Rate Constants and the Overall Equilibrium Constant at 0 and 50°.

	0°	50°
k_1 (M^{-1} sec^{-1})	4.00×10^5	1.45×10^6
k_{-1} (sec^{-1})	3.10×10^1	1.27×10^3
k_2 (M^{-1} sec^{-1})	1.51×10^3	2.59×10^6
k_{-2} (sec^{-1})	8.93×10^{-1}	3.22×10^4
k_3 (sec^{-1})	3.60×10^1	2.20×10^3
k_{-3} (M^{-1} sec^{-1})	9.26×10^7	1.75×10^6
k_4 (sec^{-1})	2.53	4.33×10^2
k_{-4}[a] (M^{-1} sec^{-1})	2.98×10^6	1.28×10^8
K_{eq}	7.20×10^{-6}	3.90×10^{-4}

[a] k_{-4} calculated from K_{eq} and the remaining rate constants.

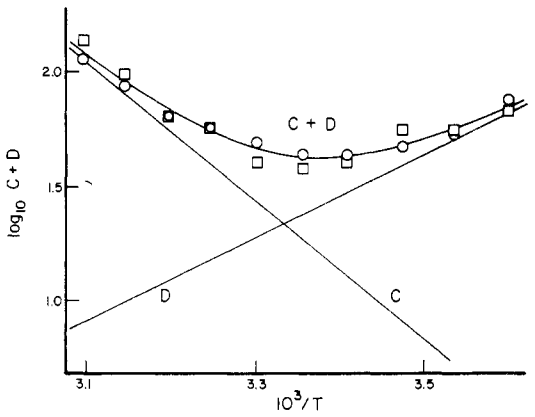

FIGURE 4: Logarithmic plot of $C + D$ against $1/T$. The circles are $K_{mX}/\bar{V}_{max}$; the squares are $K_{mB}/\bar{V}_{max}$ multiplied by $k_2k_3/k_{-2}k_{-3}$ (*cf.* eq 18).

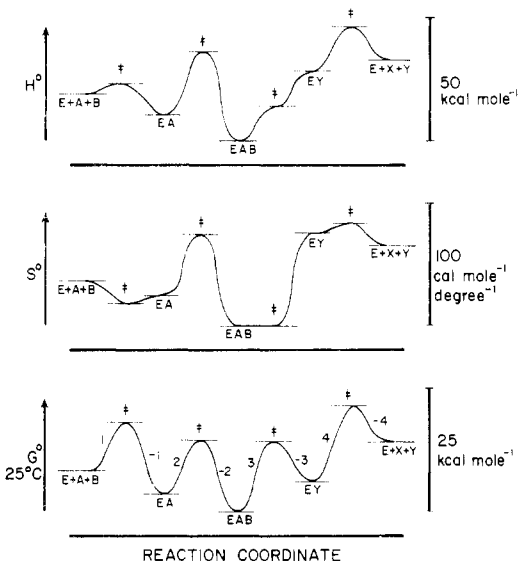

FIGURE 5: Profiles showing the changes in standard enthalpy, entropy, and Gibbs free energy at 25°.

the known k_3 gives k_{-2}; D multiplied by $k_{-2}k_{-3}/k_2k_3$ gives $1/k_2[E_0]$. Multiplication of k_{-2} by $1/k_2[E_0]$ then gives $k_{-2}/k_2[E_0]$. The line drawn in Figure 1 was based on the $k_{-2}/k_2[E_0]$ values obtained in this way, and the temperature dependence is in satisfactory agreement with that of the pre-steady-state values. Comparison of the steady-state (k_{-2}/k_2) and pre-steady-state ($k_{-2}/k_2[E_0]$) values leads to an active enzyme concentration of 5×10^{-9} M. The enzyme concentration, calculated from the protein concentration, the molecular weight (140,000), and on the assumption of 4 active sites per molecule, is 7×10^{-9} M. The agreement is very satisfactory; the fact that the kinetic procedure gives a slightly lower value than the analytical one may be explained if some of the protein is catalytically inert.

The alternative assumption that $C = k_3/k_{-2}k_{-3}[E_0]$ and $D = 1/k_{-3}[E_0]$ does not lead to a satisfactory conclusion, for two reasons. In the first place, the estimate of $k_{-2}/k_2[E_0]$ obtained on the basis of this assumption has a negative temperature dependence, inconsistent with the positive one given by the pre-steady-state data (Figure 1). Secondly, the estimated enzyme concentration is 50 times less than that given above. This alternative can therefore be discarded.

Use of this value of 5×10^{-9} M for the enzyme concentration then leads to values for k_{-1}, k_2, k_{-2}, k_3, k_{-3}, and k_4; these are given in Table I for 0 and 50°.

As explained in the Theoretical section, k_1 and k_{-4} are obtained independently of the above analysis. The constant k_1 was obtained from steady-state rates at low NAD^+ concentrations and values calculated from an Arrhenius plot are given in Table I. The overall equilibrium constant was determined directly, and its logarithmic plot against $1/T$ was linear; values at 0 and 50° are given in Table I.

The determination of k_{-4} from measurements at low NADH concentrations was not found to be satisfactory. The K_m for pyruvate decreases sharply with decreasing temperature, and at the same time a substantial amount of pyruvate inhibition was observed. It was therefore considered to be more reliable to obtain k_{-4} from K_{eq} ($=k_1k_2k_3k_4/k_{-1}k_{-2}k_{-3}k_{-4}$) and the remaining rate constants. The resulting values are included in Table I.

The values for the kinetic parameters, calculated using eq 22–24, are collected in Table II.

TABLE II: Enthalpies, Entropies, and Free Energies.

	ΔH° or $\Delta H^\ddagger$ (kcal mol^{-1})	ΔS° or $\Delta S^\ddagger$ (cal mol^{-1} dec^{-1})	ΔG° or $\Delta G^\ddagger$ at 25° (kcal mol^{-1})
k_1	4.1	−18.2	9.5
k_{-1}	12.5	−5.8	14.2
k_2	25.6	50.0	10.7
k_{-2}	36.2	74.2	14.1
k_3	13.9	−0.2	14.0
k_{-3}	−14.5	−74.8	7.9
k_4	17.5	7.6	15.2
k_{-4}[a]	12.8	17.8	7.4
k_1/k_{-1}	−8.4	−12.4	−4.7
k_2/k_{-2}	−10.6	−24.2	−3.4
k_3/k_{-3}	28.4	74.6	6.1
k_4/k_{-4}	4.7	−10.2	7.8
K_{eq}	14.1	27.8	5.8

[a] k_{-4} calculated from $k_1k_2k_3k_4/k_{-1}k_{-2}k_{-3}$ divided by K_{eq}.

Discussion

The rate constants k_1, k_3, k_4, and k_{-1} (assuming $\bar{V}_{max}$ to be equal to $k_1[E_0]$) and the equilibrium constants k_2/k_{-2}, $k_2k_3/k_{-2}k_{-3}$, and K_{eq} have been determined directly and are therefore quite reliable; the energies associated with these quantities are therefore expected to be correct within a kilocalorie or so. The constants k_2, k_{-2}, k_3, and k_{-4} have been calculated indirectly and are therefore dependent on the accuracy of the model used. Any of the latter four constants could in fact be products of rate constants and equilibrium constants for reaction steps not included in our model.

Thermodynamics. Figure 5 shows an energy profile for the enthalpy, entropy, and Gibbs free energy changes at 25°. The free energy profiles for 0 and 50° are shown for comparison in Figure 6; in this diagram the levels for EAB are arbitrarily taken to be the same, in order for the differences to be displayed more clearly. An interesting feature of Figures 5 and 6 is that EAB has a lower standard free ener-

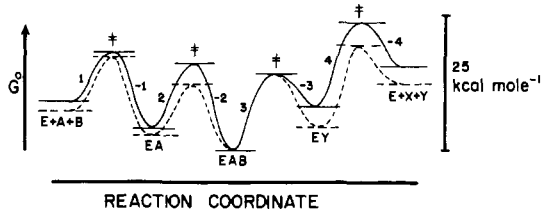

FIGURE 6: Standard Gibbs free energy profile at 0° (—) and 50° (- - -).

gy than any of the other species. This means that under standard conditions (unit concentrations) the ternary complex EAB will be predominant. The entropy diagram (Figure 5) also shows that EAB is the species of minimum entropy, which probably means that it is the most folded form; as such, it may well be the most resistant to denaturation.

In connection with the thermodynamic values for the species E, EA, EAB, and EX, it is to be noted from Figure 5 that all of the binding processes (E + A → EA; EA + B → EAB; E + Y → EY; and EY + X → EAB) are exothermic and exergonic. Moreover, all of these processes except E + Y → EY involve a decrease in entropy. The equilibria for the binding processes other than E + Y → EY are therefore dominated by the enthalpy changes. The binding of Y (NADH), on the other hand, is partly due to the loss in enthalpy and partly to the gain in entropy. The complex EY has a higher entropy than E, EA, and EAB, which suggests that it is the most unfolded form; addition of NADH to E, in other words, has an important unfolding effect. NADH has considerably more enthalpy than NAD^+ (EY has a much higher enthalpy than EA), and some of its energy results in unfolding of the enzyme.

In considering the thermodynamical changes that are involved in the formation of the various activated complexes, we may note at the outset that the enthalpy of activation associated with reaction −3 (EY + X) is negative. This is a somewhat unusual circumstance, but the corresponding entropy of activation is also strongly negative, so that the free energy of activation is positive. There is therefore no theoretical difficulty, and we have support for the point of view (Laidler, 1969) that activated complexes are to be considered to exist at the maxima of free-energy and not of enthalpy barriers. It is to be noted that in this reaction, the addition of pyruvate to E:NADH, there is the addition of a proton, which then combines with H^- from the NADH to convert pyruvate to lactate. It is possible that the large entropy loss in reaction −3 is associated with this protonation process.

Other reactions having negative entropies of activation are 1 and −1; addition or release of NAD^+ to the enzyme thus presumably leads to a more folded structure. Associated with these negative entropies of activation are rather low enthalpies of activation, so that the processes have fairly low free-energy barriers and occur at reasonable speeds. The folding process perhaps puts the enzyme into a conformation in which the activation energy requirement is less stringent.

Reaction 3 occurs with zero entropy of activation, so that there is little conformational change when the pyruvate molecule leaves the ternary complex. As a result of this, the free energy of activation for this process is independent of temperature (Figure 6).

By contrast, the entropies of activation associated with reactions 2, −2, 4, and −4 are all positive. This implies that addition or release of either lactate or NADH produces an activated complex that is more unfolded than the reactants. The positive entropies of activation lead to an increase in the rates of these processes, all of which have fairly high activation energies. It is to be noted that, as is common, there is something of a compensation effect, high activation energies tending to be associated with high entropies of activation, so that the free-energy barriers for all of the eight reactions do not vary widely.

The curvature in the K_m plots for lactate and pyruvate results from the large difference between the entropies of activation for reactions −2 and 3. Since the entropy of activation for reaction 3 is very small, the free energy of activation is almost independent of temperature. The free energy of activation for reaction −2, however, is more strongly dependent on temperature. As a result, the free energy of activation for −2 is lower than that for 3 at higher temperatures, but is higher at lower temperatures.

Biological Implications. Since physiological substrate concentrations are almost always too low to saturate enzymes (Hochachka and Somero, 1973), the reaction rate at low (below or equal to K_m) substrate concentrations is more significant than at high substrate concentrations. Since the value of V_{max}/K_m is closer to the true reaction velocity than is V_{max}, whenever the substrate concentration is below K_m, the ratio V_{max}/K_m has a greater biological significance than does V_{max}.

The temperature dependence of $\bar{V}_{max}/K_m$ for NAD^+ is smaller than the temperature dependence for V_{max}. This is shown by the lower enthalpy of activation for k_1 than for k_4. The same phenomenon was observed by Harbison and Fisher (1973a,b) for adenosine deaminase from molluscs. The reaction mechanism proposed for this enzyme was the same as that used in this paper with A = adenosine and B = H_2O. The V_{max} showed a strong temperature dependence and V_{max}/K_m showed essentially no temperature dependence. Both V_{max} and V_{max}/K_m produced linear Arrhenius plots, as do V_{max} and V_{max}/K_{mA} for lactate dehydrogenase.

Unlike the enthalpy of activation for reaction 1, that for −4 (k_{-4} is proportional to the rate in the reverse direction at low NADH concentrations) is much larger, and from our indirect calculations appears to be approximately as large as k_{-1}.

The values of $\bar{V}_{max}/K_{mB}$, along with $\bar{V}_{max}/K_{mX}$, are shown in Figure 7. The points are the experimentally observed values and the curves are calculated using the values in Table I. At low temperatures, k_3 is much greater than k_{-2} so that the reaction rate in the forward direction is proportional to $k_2[E_0]$ (note the similarity to $\bar{V}_{max}/K_{mA} = k_1[E_0]$). At high temperatures, k_{-2} is much larger than k_3 and the rate is proportional to k_3 times the concentration of the intermediate EAB. EAB is proportional to k_2/k_{-2} and the reaction rate is therefore proportional to $(k_2k_3/k_{-2})[E_0]$.

A similar argument can be made for $\bar{V}_{max}/K_m$ for pyruvate. At high temperatures this value is approximately equal to $k_{-3}[E_0]$. Since k_{-3} decreases with an increase in temperature, the reaction rate at low pyruvate concentrations goes through a maximum at about 20–25°. The complete reversal of the temperature dependence of $\bar{V}_{max}/K_{mX}$ is due to the extremely strong temperature dependence of K_{mX} as well as its nonlinearity on an Arrhenius plot.

It has been stated that V_{max}/K_m for the ternary complex mechanism (second substrate) and the Michaelis-Menten

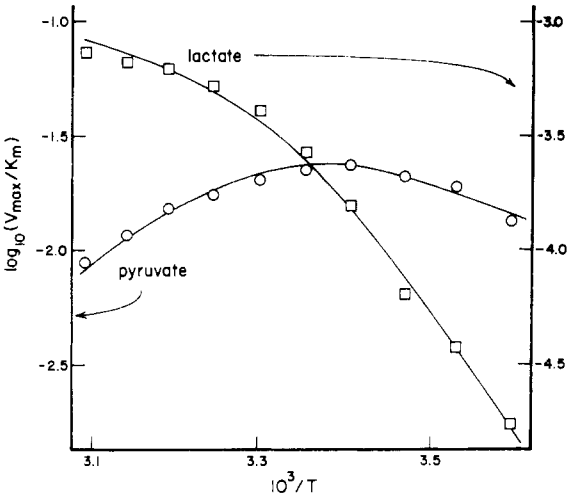

FIGURE 7: Logarithmic plots of V_{max}/K_m against $1/T$ for the reactions in forward and reverse directions.

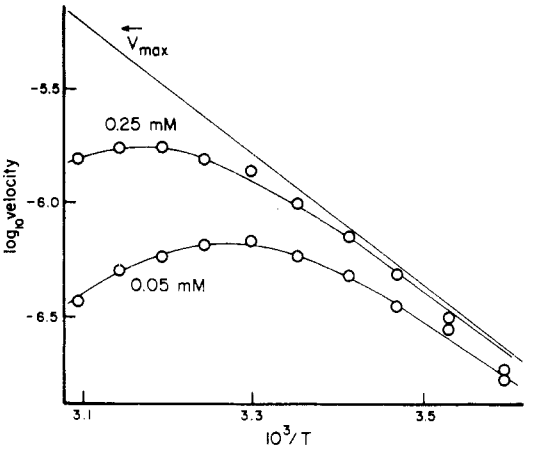

FIGURE 8: Logarithmic plots of velocity in the reverse direction (pyruvate → lactate) against $1/T$, at two pyruvate concentrations. The curves represent values calculated from eq 26; the points are experimental.

mechanism are equivalent. Both give nonlinear Arrhenius plots. This is because the rate at low substrate concentrations can be proportional either to the rate of addition of substrate (k_2 for lactate and k_{-3} for pyruvate) or the step following (k_3 for lactate and k_{-2} for pyruvate). On the other hand, $\tilde{V}_{max}/K_{mA}$ is proportional only to the rate of addition of substrate (k_1). Reaction 2 is never rate limiting when $\tilde{V}_{max}/K_{mA}$ is being determined because saturating concentrations of the second substrate are being used, which makes this step fast. Consequently, V_{max}/K_m for NAD^+ or NADH will obey the Arrhenius law when saturating concentrations of lactate or pyruvate are used.

The value of the reaction velocity in the reverse direction has been calculated from

$$\nu = \tilde{V}_{max}(\text{pyruvate})/[K_{mX} + (\text{pyruvate})] \quad (25)$$

with saturating NADH and two different pyruvate concentrations (0.05 and 0.25 mM). The calculated curve is shown in Figure 8 and, as before, the points represent actual data. At physiological pyruvate concentrations (0.05 mM; Lehninger, 1970) the enzyme is almost completely saturated at low temperatures but the substrate concentration is well below K_m at high temperatures (see Figure 8). The reaction thus goes through a maximum at about 30–35°, which is remarkably close to the 35–40° body temperature range for most endothermic (warm-blooded) animals.

These observations for lactate dehydrogenase from an endothermic organism would predict that the homologous enzyme from an ectothermic (cold-blooded) organism, with a much lower body temperature, would show a maximum at a lower temperature. It is also possible that the energy profiles for such an enzyme might be altered. A similar suggestion has been made by Low *et al.* (1973). Further research is now in progress establishing individual rate constants and thermodynamic parameters for lactate dehydrogenase isolated from an ectotherm.

References

Glasstone, S., Laider, K. J., and Eyring, H. (1941), The Theory of Rate Processes, New York, N. Y., McGraw-Hill, pp. 197–199.

Harbison, G. R., and Fisher, J. R. (1973a), *Comp. Biochem. Physiol. B 46,* 283.

Harbison, G. R., and Fisher, J. R. (1973b), *Comp. Biochem. Physiol. B 47,* 27.

Hijazi, N. H., and Laidler, K. J. (1973a), *Can. J. Biochem. 51,* 815.

Hijazi, N. H., and Laidler, K. J. (1973b), *Can. J. Biochem. 51,* 832.

Hochachka, P. W., and Somero, G. N. (1973), Strategies of Biochemical Adaptation, Toronto, W. B. Saunders Co., p 11.

Holbrook, J. J., and Gutfreund, H. (1973), *FEBS (Fed. Eur. Biochem. Soc.) Lett. 31,* 157.

Laidler, K. J. (1965), Chemical Kinetics, 2nd ed, New York, N. Y., McGraw-Hill, Co., pp 88–90.

Laidler, K. J. (1969), Theories of Chemical Reaction Rates, New York, N. Y., McGraw-Hill, pp 76–79.

Laidler, K. J., and Bunting, P. S. (1973), The Chemical Kinetics of Enzyme Action, Oxford, Clarendon Press, pp 341–351.

Lehninger, A. L. (1970), Biochemistry, New York, N. Y., Worth Publishers Inc., p 327.

Low, P. S., Bada, J. L., and Somero, G. N. (1973), *Proc. Nat. Acad. Sci. U. S. 70,* 430.

Maguire, R. J., Hijazi, N. H., and Laidler, K. J. (1974), *Biochim. Biophys. Acta 341,* 1.